Improved prediction model for time-dependent deformations of concrete: Part 1-Shrinkage

ZDENĚK P. BAŽANT, JOONG-KOO KIM

Center for Advanced Cement-Based Materials, Northwestern University, Evanston, Illinois 60208, USA

LIISA PANULA†

TAMS, New York, NY 11003, USA

This paper is the first in a series of papers that present a new prediction model for creep and shrinkage of concrete, called for brevity the BP-KX model. This model represents an update and improvement of the BP model published in this journal in 1978–79. The improvement is possible because further experimental data became available in the literature and at the same time knowledge of physical concepts and mechanisms has improved. This first paper presents a prediction model for the mean (overall) shrinkage strain in cross-sections of long members, which takes into account the influence of environmental humidity, the effective thickness of the member, the effect of cross-section shape, the effect of age at the start of drying, and the effect of temperature. The proposed basic form of the shrinkage formulae is justified by non-linear diffusion theory for the movement of moisture through concrete. Extensive comparisons with important test data from the literature, altogether 23 data sets, reveal that the predictions are better than with the previous models. Statistics of prediction are also given. The main error of prediction arises from the estimation of the shrinkage parameters from concrete strength and composition. If limited short-time shrinkage data are available, the predictions can be greatly improved.

1. INTRODUCTION

Creep and shrinkage of concrete may significantly reduce the safety margins against some types of collapse, particularly creep buckling, and have a major effect on the durability of concrete structures. Mispredictions of deflections of bridges, as well as stresses and cracking engendered by shrinkage and non-uniform creep, are one major cause of inadequate durability of many structures. If, for example, bridges designed for a life-span of 50 years have to be closed for major repairs or replaced because of cracking or excessive deflections after 40, 30 or only 20 years, the economic cost is tremendous. Considering all the repairs and premature closings of concrete structures, the costs to the national economies are truly staggering. Therefore it pays to give careful attention to creep and shrinkage.

More than a decade ago, an innovative and relatively sophisticated practical prediction model for creep and shrinkage was presented [1]. This model, which later became known as the BP model, was to a larger extent based on physical considerations and mathematical arguments than the preceding models and proved to give much better predictions. At the same time, this model was more complex than others, which some engineers considered objectionable. However, the question of model complexity must be judged in relative terms.

Computer evaluation of the creep and shrinkage values by any model is fast and cheap, compared to finite-element analysis, for example. Even for hand calculation, the fact that evaluation from the BP model takes about four hours while for some other model it may take only half an hour is insignificant for a structural engineer who has no objection to spending many days on finite-element analysis of a structure. At the same time, if one considers a creep-sensitive structure, the error caused by replacing the BP model by some simplistic model is many times larger than the error caused by replacing finite-element analysis with an old-fashioned hand calculation under over-simplifying assumptions. In this light, none of the existing models can be judged as too complex for practice.

A sophisticated creep prediction model is of course necessary only for creep-sensitive structures, e.g. a large-span prestressed concrete bridge, a nuclear containment, a large-span roof shell or a tall building. Creep-insensitive structures, for example a simply supported unprestressed reinforced concrete beam, can of course be analysed adequately even by simplistic models. However, it is important to decide rationally whether a more realistic and sophisticated prediction model is needed. This decision should be based on statistics, particularly calculation of the coefficients of variation of the structural effects of creep and shrinkage. The method of calculating these is known quite well (e.g. [2]) and is not much more difficult that calculation of the mean predictions of

† Deceased 1989.

structural effects. For this purpose every prediction model should include information on the coefficient of variation of the predicted creep and shrinkage values. This can be adequately determined only by statistical comparisons with the existing experimental data in the literature, as pioneered in the original presentation of the BP model (all the important data must be used; how a selective use of only some data can yield misleading conclusions about the model errors has already been documented [1]). Such statistical information ought to be given for every prediction model, even a very simple one. Then the engineer can determine whether, for instance, a coefficient of variation of 80% of the creep coefficient has a negligible effect or an important effect on the structure. From this he can decide whether it is worthwhile to stay with the simplest model or switch to a more realistic one. Such an approach would eliminate the arguments as to what level of sophistication is needed for code recommendations. Models of several levels of sophistication could be recommended side by side, provided that information on the error of each is given. The designer should be free to choose the simplest model whose error is to him tolerable.

Since the original development of the BP model further important experimental data have appeared in the literature, and also the knowledge of physical mechanisms and the mathematical formulation of creep or shrinkage has progressed. Therefore efforts to improve and update the original BP model have been undertaken and their results will be presented in a series of papers dealing with the prediction of (i) shrinkage, (ii) basic creep, (iii) drying creep, (iv) temperature effect on basic creep, (v) temperature effect on drying creep, and (vi) effects of cyclic stress and cyclic humidity. For the sake of distinction from the original BP model, the present model will be called the BP-KX model.

The present work will also serve the secondary purpose of compiling, organizing and summarizing the existing test data on creep and shrinkage into a comprehensive databank. Availability of this databank should save much tedious work to anyone who intends to evaluate any other prediction model. Even for very simple models, comparison with all the present data is necessary to determine the coefficients of variation of their statistical errors.

2. SCOPE OF APPLICABILITY

The BP-KX model that will be presented in the series of papers that follows is applicable to a broad range of concretes. Best accuracy is obtained for normal concretes of 3000 to 9000 psi (21 to 62 MPa) cylindrical compression strength, with neither admixtures nor superplasticizers. Although most data used to verify and calibrate the model pertain to normal concretes, limited data show that the model is applicable, albeit with greater errors, to high-strength and lightweight concretes as well. As for concretes with admixtures or superplasticizers, the creep and shrinkage equations seem to be also approximately

applicable to such concretes, but their six basic parameters $(\varepsilon_{s\infty}, q_1, \dots, q_5)$ must be calibrated by tests; the formulae for predicting these material parameters from concrete strength and composition are not applicable to such concretes.

3. SHRINKAGE PROBLEM

Two types of shrinkage must be distinguished: (i) free shrinkage and (ii) mean shrinkage in the cross-section of a structural member, e.g. a wall or a long prismatic member. Only the latter type of shrinkage, which is needed for the analysis of beams, frames and plates, will be addressed here. The free shrinkage is the shrinkage of a very small material element whose moisture content remains almost uniform during drying. The free shrinkage is much simpler to characterize mathematically, but is much more difficult to determine from experimental observations and usually more difficult to use in structural analysis. Free shrinkage can be directly measured only on extremely thin specimens exposed to very slowly varying environmental humidity [3]. The free shrinkage is what is needed for two- and three-dimensional or layered finite-element analysis, while the mean or overall cross-section shrinkage is what is needed for the analysis of structures by beam theory, including beam-type finite elements.

In a rigorous and fully realistic approach the prediction of shrinkage deformations of concrete members and structures is a truly formidable problem. It requires solving the diffusion equation for the movement of water through the pores of concrete, driven by gradients of pore relative humidity. The diffusion flux is affected by cracking and microcracking which may be produced by non-uniform shrinkage as well as other types of loads. Knowing the distribution of pore relative humidity or relative moisture content throughout the structure at all times, one can calculate the free shrinkage which would occur in unrestrained material elements. However, such free shrinkage strains are incompatible, and therefore residual stresses, called shrinkage stresses, develop. They are of long duration and therefore produce significant creep. This creep is strongly affected by the simultaneous changes of moisture content at each material element, as well as by ageing due to the progress of hydration. The ageing rate depends on the moisture content and temperature. Creep causes relaxation and redistribution of internal stresses, which are beneficial to structural performance. In spite of the shrinkage stress relaxation due to creep, shrinkage stresses cause cracking which may localize into large fractures depending on structure size and geometry, and stored energy. The tendency to crack and localize is opposed by reinforcement, which may completely prevent the formation of large visible cracks. Due to the action of reinforcement, bond slip may also affect shrinkage. Simultaneous temperature changes have a great effect on the magnitude of shrinkage, as well as on the movement of moisture and the creep that relaxes the shrinkage stresses.

Shrinkage analysis that takes all the foregoing

phenomena into account recently became feasible, by means of finite elements, and the approximate material laws required for such analysis have been established. However, to avoid the complexity of such analysis, there continues to be a strong need for prediction formulae for the mean shrinkage in the cross-section of a concrete member. We present such formulae now. In discussing them, we focus in this paper series on those aspects that differ from the BP model. For the discussion of those aspects that are similar, the reader may consult Bažant and Panula [1].

4. PREDICTION FORMULAE

Mean shrinkage strain in the cross-section:

$$\varepsilon_{sh}(t, t_0) = \varepsilon_{sh\infty} k_h S(\hat{t}) \qquad \hat{t} = \int_{t_0}^{t} k_T'(t'')\,dt'' \qquad (1)$$

Time curve:

$$S(\hat{t}) = \tanh\left(\frac{\hat{t}}{\tau_{sh}}\right)^{1/2} \qquad (2)$$

Humidity dependence:

$$k_h = \begin{cases} 1 - h^3 & \text{for } h \le 0.98 \\ -0.2 & \text{for } h = 1 \\ \text{linear interpolation} & \text{for } 0.98 \le h \le 1 \end{cases} \qquad (3)$$

Size dependence:

$$\tau_{sh} = \frac{0.32(k_s D)^2}{C_1(t_{0e})} \qquad D = \frac{2v}{s} \qquad (4)$$

Shape dependence:

$$k_s = \begin{cases} 1.0 & \text{for an infinite slab} \\ 1.15 & \text{for an infinite cylinder} \\ 1.25 & \text{for an infinite square prism} \\ 1.30 & \text{for a sphere} \\ 1.55 & \text{for a cube} \end{cases} \qquad (5)$$

Age dependence:

$$C_1(t_0) = C_0\left[0.6 + \left(\frac{4.5}{t_{0e}}\right)^{1/2}\right]$$

$$\text{with } C_0 = 10, \text{ but } C_1(t_0) \le 18 \qquad (6)$$

$$\varepsilon_{sh\infty} = \varepsilon_{s\infty}\left[G\left(17 + \frac{\tau_{sh}}{40}\right)G(12 + t_{0e})\right]^{-1} \qquad (7)$$

where

$$t_{0e} = \begin{cases} 25 + t_0 & \text{for a steam-cured specimen} \\ t_0 & \text{otherwise} \end{cases} \qquad (8)$$

$$G(x) = \left(\frac{x}{4 + 0.9x}\right)^{1/2} \qquad (9)$$

Temperature dependence:

$$k_T' = \exp\left[\frac{Q}{R}\left(\frac{1}{T_0} - \frac{1}{T}\right)\right] \qquad \frac{Q}{R} = 5000\,\text{K} \qquad (10)$$

Here t = time (in days), representing the age of concrete; t_0 = age when drying begins; t_{0e} = effective age (maturity)

when drying begins: $\hat{t} = t - t_0$ = duration of drying; $\varepsilon_{sh\infty}$ = ultimate shrinkage; h = relative humidity of environment $(0 \le h \le 1)$; τ_{sh} = shrinkage half-time; D = effective cross-section thickness in millimetres; v/s = volume-to-surface ratio in millimetres; $C_1(t_0)$ = drying diffusivity of nearly-saturated concrete at reference temperature; k_T' = temperature coefficient based on the activation energy of moisture migration [4]; Q = activation energy; R = gas constant; k_s = shape factor [5]; T = temperature of specimen; and T_0 = reference temperature (chosen as 23°C for all the tests). In Equation 10, T and T_0 must be given in degrees Kelvin (absolute temperatures).

The k_s value for a cylinder or prismatic specimen of finite length may be obtained by interpolating between the value for a sphere or cube and the value for an infinitely long specimen, which can be used when the length of beam is at least three times its width. For $h = 1.0$ the function of k_h gives swelling under water, and for $h = 0.98$ it roughly gives the autogenous shrinkage of standard specimens (here the typical pore humidity caused by self-desiccation in sealed specimens is assumed to be 0.98).

5. PREDICTION OF MATERIAL PARAMETERS FROM COMPOSITION AND STRENGTH

The problem of predicting the parameters of concrete shrinkage and creep formulae from concrete mix composition and strength of concrete is much harder than the establishment of the formulae themselves, and inevitably involves a much larger error. This error can be eliminated only by shrinkage measurement. In the absence of any measurements, the following empirical formulae need to be used for the final shrinkage (in 10^{-3}):

$$\varepsilon_{s\infty} = (1.15\alpha_1 + 0.16)\alpha_2\alpha_3 \qquad (11)$$

where

$$\alpha_1 = \left(\frac{w}{c}\right)^{1.5} c^{1.1} f_c'^{-0.2}\left(1 - \frac{a}{\rho_c}\right)\alpha_4 \qquad (12)$$

$$\alpha_4 = \begin{cases} 0.7 + 0.3(a/s - 1.6)^{-3} & \text{for } a/s > 2.6 \\ 1 & \text{otherwise} \end{cases} \qquad (13)$$

$$\alpha_2 = \begin{cases} 1.0 & \text{for type I} \\ 0.85 & \text{for type II} \\ 1.1 & \text{for type III} \end{cases} \qquad (14)$$

$$\alpha_3 = \begin{cases} 1.0 & \text{for specimens cured in water or 100\% RH} \\ 1.4 & \text{for specimens sealed during curing} \\ 0.74 & \text{for steam-cured specimens} \end{cases} \qquad (15)$$

Here c = cement content in lb ft^{-3} (16 kg m^{-3}); w/c = water/cement ratio; f_c' = 28-day cylinder strength in psi (6.9 kPa); a/ρ_c = aggregate/concrete density ratio; and a/s = aggregate/sand ratio. Sand is defined as aggregate passing through a No. 4 (4.7 mm) sieve; the larger aggregates are considered as gravel.

The basic qualitative trends reflected in these formulae are as follows: (a) a stronger concrete shrinks less; (b) increasing the water/cement ratio and cement content

while maintaining the same strength results in higher shrinkage; and (c) the ultimate shrinkage for the same strength decreases with an increase in the aggregate/concrete density ratio.

The mineralogical type of the aggregates does not appear explicitly, but it enters the calculations indirectly through the value of the elastic modulus of concrete and the strength of concrete, which depend on the mineralogical type of the aggregate. Unfortunately many of the data-sets used in the study do not include information on the type of aggregate, and thus it is impossible to determine influences of the mineralogical type other than those that arise through the elastic modulus and strength.

6. IMPROVEMENT OF PREDICTION BASED ON LIMITED SHORT-TIME TESTS

The prediction error due to Equations 11–15 is much larger than that due to Equations 1–10. It must be emphasized, however, that the error of prediction can be greatly reduced if at least some limited-duration tests of shrinkage are made for the concrete under consideration.

If such tests are very limited (one week duration, thin specimens), one first predicts all the parameters from Equations 11–13. Then one replaces

$$\varepsilon_{s\infty} \leftarrow r\varepsilon_{s\infty} \tag{16}$$

Coefficient r is then determined so as to obtain an optimum fit of the measured data.

If the results of at least one month duration are available, one can update two parameters, $\varepsilon_{s\infty}$ and C_0. First one predicts all the parameters from Equations 11–13. Then one replaces $\varepsilon_{s\infty}$ and C_0:

$$\varepsilon_{s\infty} \leftarrow r_1\varepsilon_{s\infty} \qquad C_0 \leftarrow r_2 C_0 \tag{17}$$

Coefficients r_1 and r_2 are then determined so as to obtain an optimum fit of the data. To do that a trial-and-error approach is possible, but a non-linear optimization subroutine is more efficient.

7. COMPARISON WITH SHRINKAGE TEST DATA

First it has been checked that Equations 1–10, without material parameter predictions (Equations 11–15), can give very close fits of the extensive test data in the literature. This verifies that the mathematical form of the model is satisfactory. Then, by minimizing the sum of squared deviations from test data, the present model with material parameter predictions (Equations 11–15) has been calibrated so as to give optimum fits of 23 different data-sets from the literature, exhibited in Figs 1 to 8. For the method of fitting and optimization, see Bažant and Panula [1].

The most comprehensive and consistent data-sets are those of Keeton [6], Kesler et al. [7] and Wallo et al. [8]. As for the size effect, the data of Hansen and Mattock [9] are most relevant. The negative values of the data on the massive specimens in L'Hermite and Mamillan's shrin-

kage tests [10], which are shown in Fig. 5, are probably due to the effect of thermal expansion caused by hydration heat, which is not included in Equations 1–15. For the statistical calculation of the coefficient of variation, the data-sets that include negative values were ignored. Some tests of L'Hermite et al. [11] were conducted under water (e.g. swelling) but these data-sets were ignored in the statistical analysis for the coefficient of variation (Fig. 5). The tests of Hummel et al. [12] include five different w/c ratios and two different types of cement, but the data that pertain to $w/c = 0.65$ were excluded because the trend of shrinkage versus w/c in these data was opposite to that generally observed. The carefully controlled tests reported by Wittmann et al. [13], which involved large numbers of identical specimens, were essential for establishing the time curve (Equation 2). The data of Rüsch et al. [14], which have different but very close s/c and g/c, were averaged because there is lack of information on the properties of the aggregates.

The tests of Dreux and Gorisse [15] dealt with reinforced prisms. The corresponding shrinkage ε_{sh} for unreinforced prisms shown in Fig. 1 was estimated from these data as $\varepsilon_{sh} = \varepsilon/(1 + pE_s/E_c'')$, where ε = measured strain, p = reinforcement ratio, E_s = elastic modulus of steel and E_c'' = age-adjusted effective modulus (given by Equation 5 of Bažant [16] and Bažant et al. [17]). The ratio $\varepsilon/\varepsilon_{sh}$ was about 0.97, so any possible inaccuracy of the correction method must have been insignificant.

From the tests of Hilsdorf [18], which include six different data-sets, five with cylinders and one with prisms, the data obtained for specimens exposed at $t_0 = 1$ and 90 days were excluded because the trend of shrinkage change with t_0 in these data was opposite to that required by accepted laws. Also one data-set from Ngab et al. [19,20] was excluded from analysis because its values were inexplicably low compared with the data for other specimens that had very close composition and strength. The tests of Espion and Wastiels [21] show the scatter of three sets of tests which have the same composition but slightly different strengths. The tests of Troxell et al. [22] also include data on swelling, but for statistical analysis those data were also neglected. In the tests of Wesche et al. [23] the measured data in Fig. 7 (Wesche et al. (c) at $t_0 = 7$ days) were averaged.

The basic information pertaining to the test data used is summarized in the Appendix. Some of this information was not included in the original publications but has been obtained personally from the respective authors.

The temperature factor k_T' in Equation 10 cannot be confirmed by the existing shrinkage data because their range of temperatures is very narrow. This factor will be calibrated later from drying creep formulae.

8. STATISTICS OF ERRORS OF PRESENT MODEL

Having proposed prediction formulae for shrinkage, we now indicate the accuracy of its predictions, characterized by the coefficients of variation $\bar{\omega}$ of the deviations of the
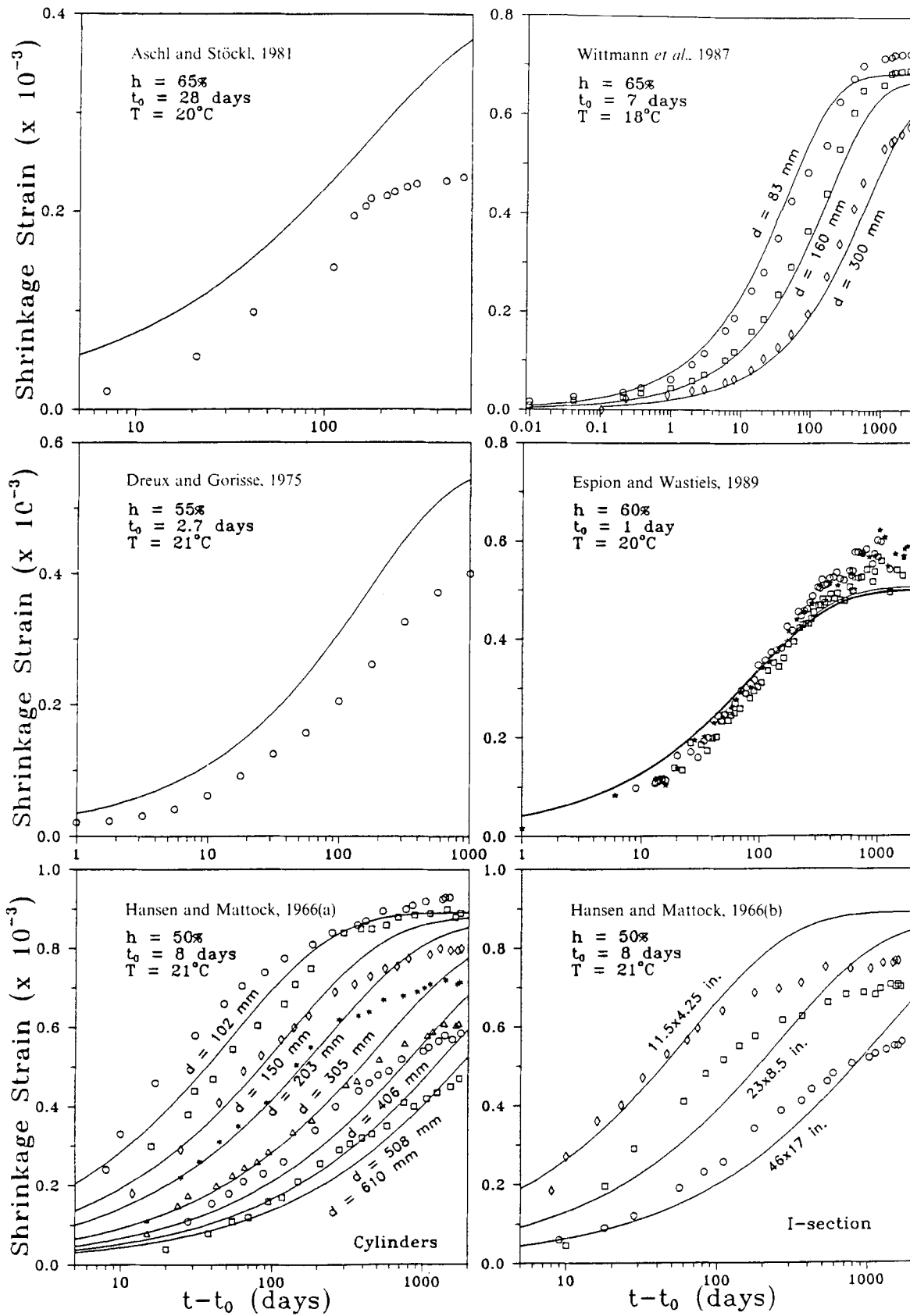
Fig. 1 Predictions of shrinkage and data by Aschl and Stöckl, Wittmann *et al.*, Dreux and Gorisse, Espion and Wastiels, and Hansen and Mattock.
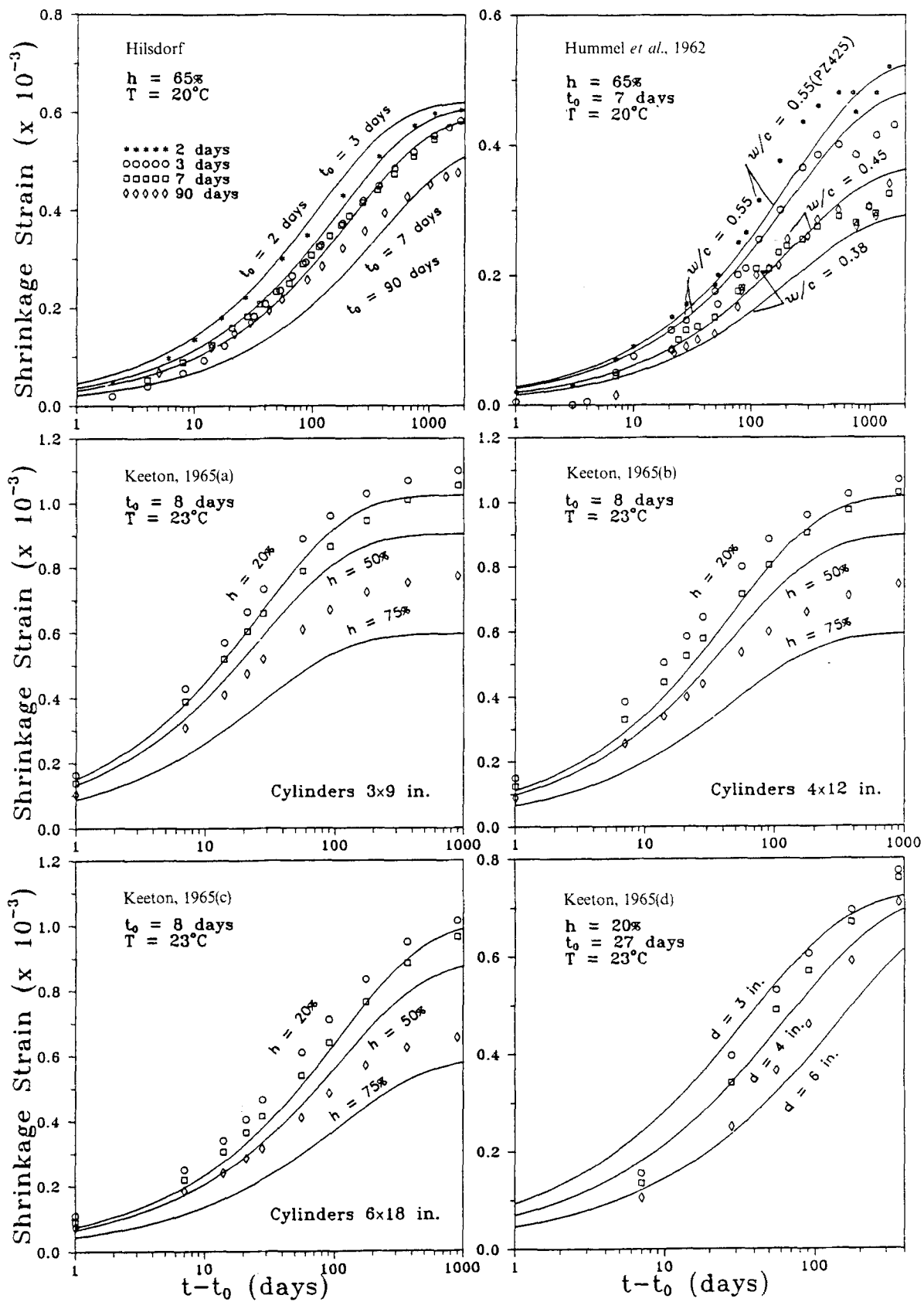
Fig. 2 Predictions of shrinkage and data by Hilsdorf, Hummel *et al.* and Keeton.
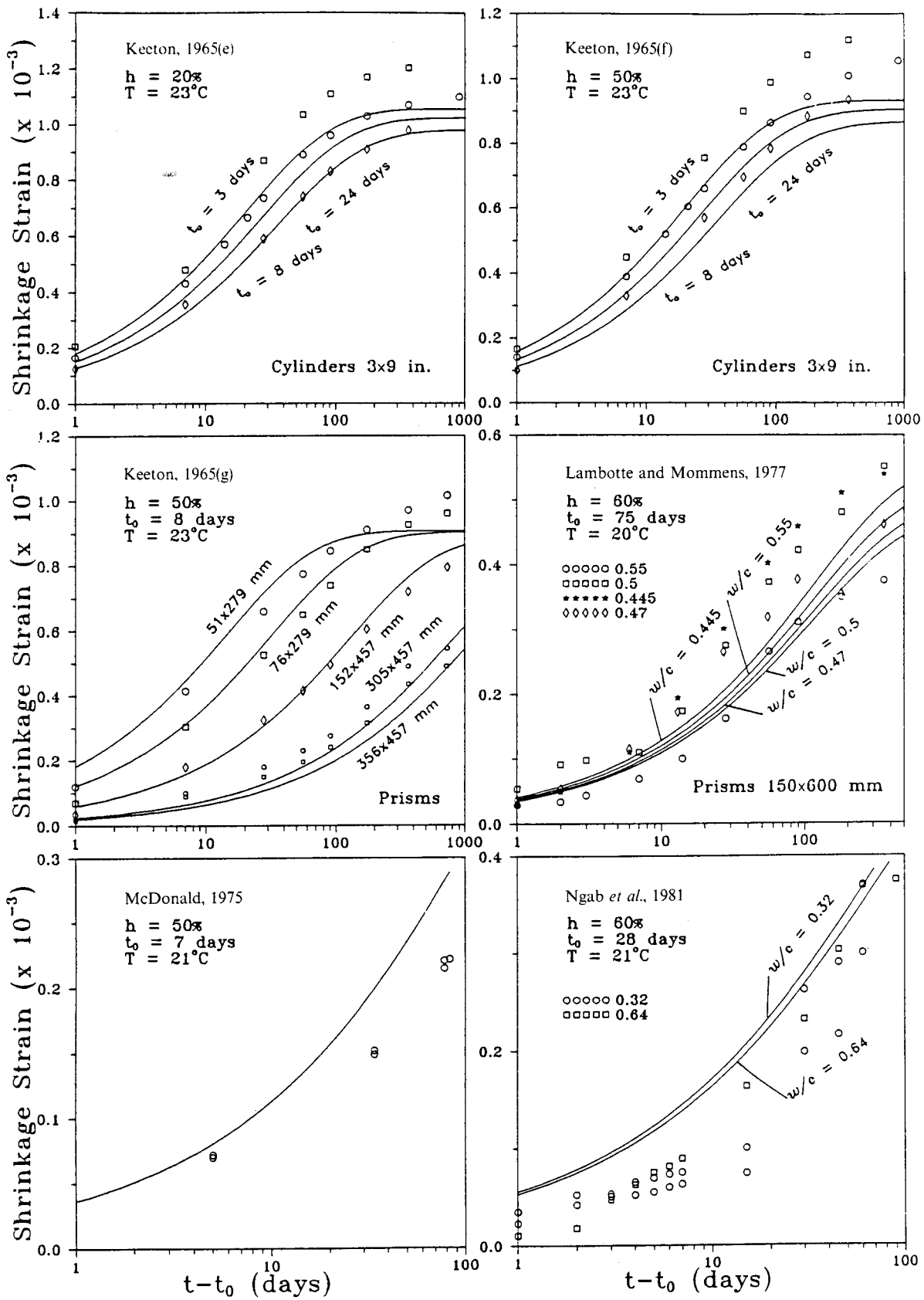
Fig. 3 Predictions of shrinkage and data by Keeton, Lambotte and Mommens, McDonald and Ngab *et al.*
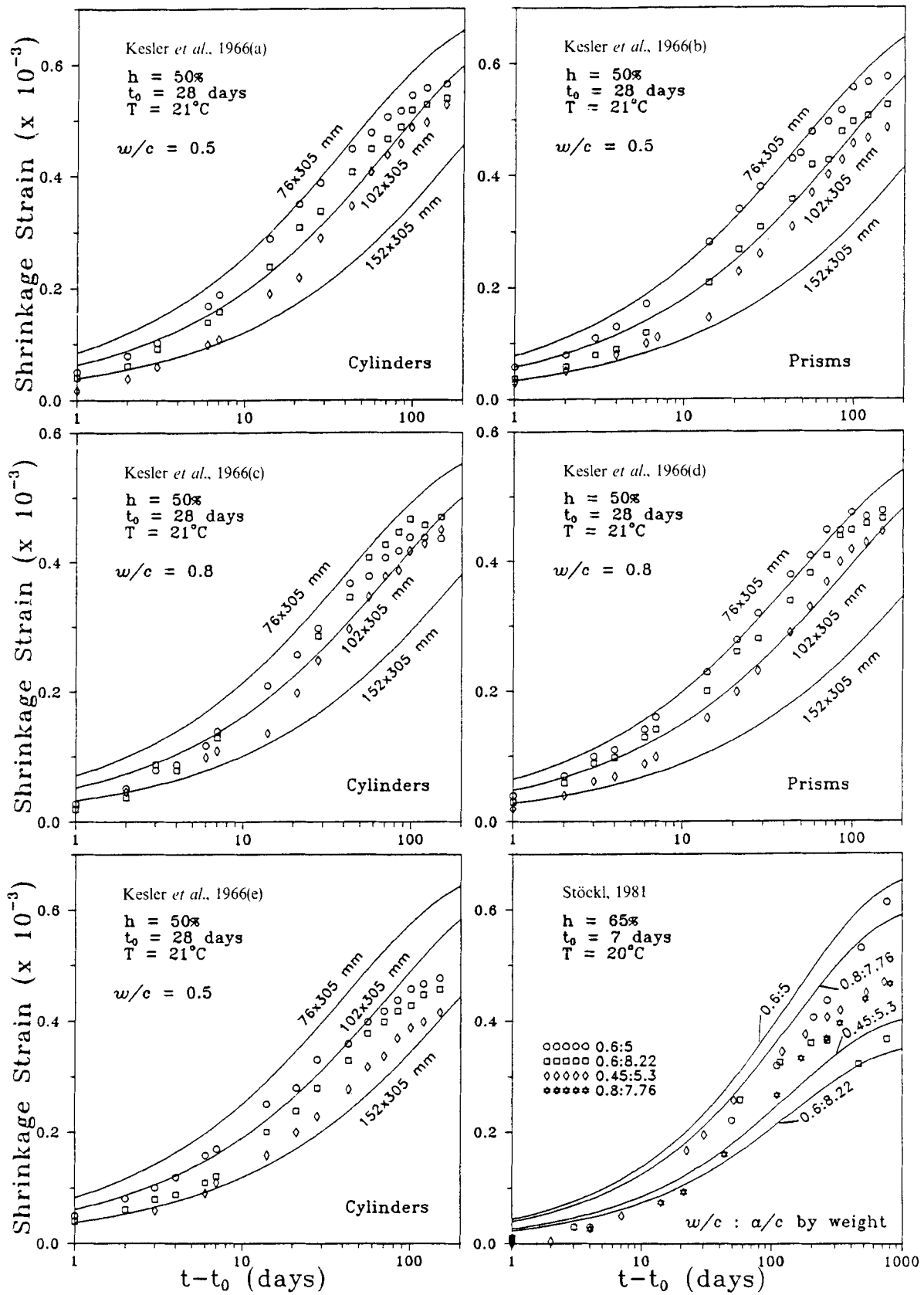
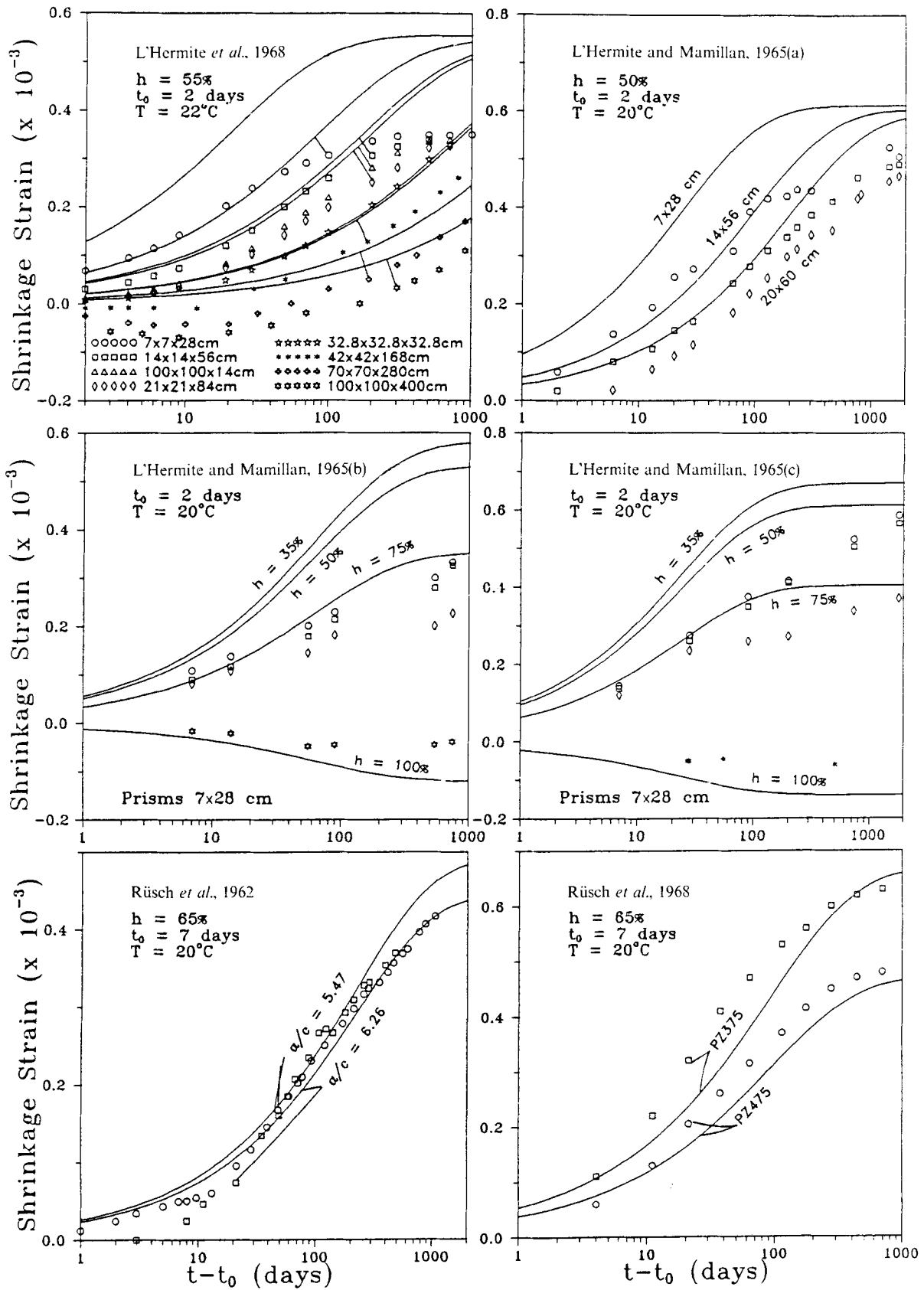Fig. 4 Predictions of shrinkage and data by Kesler et al. and Stöckl.

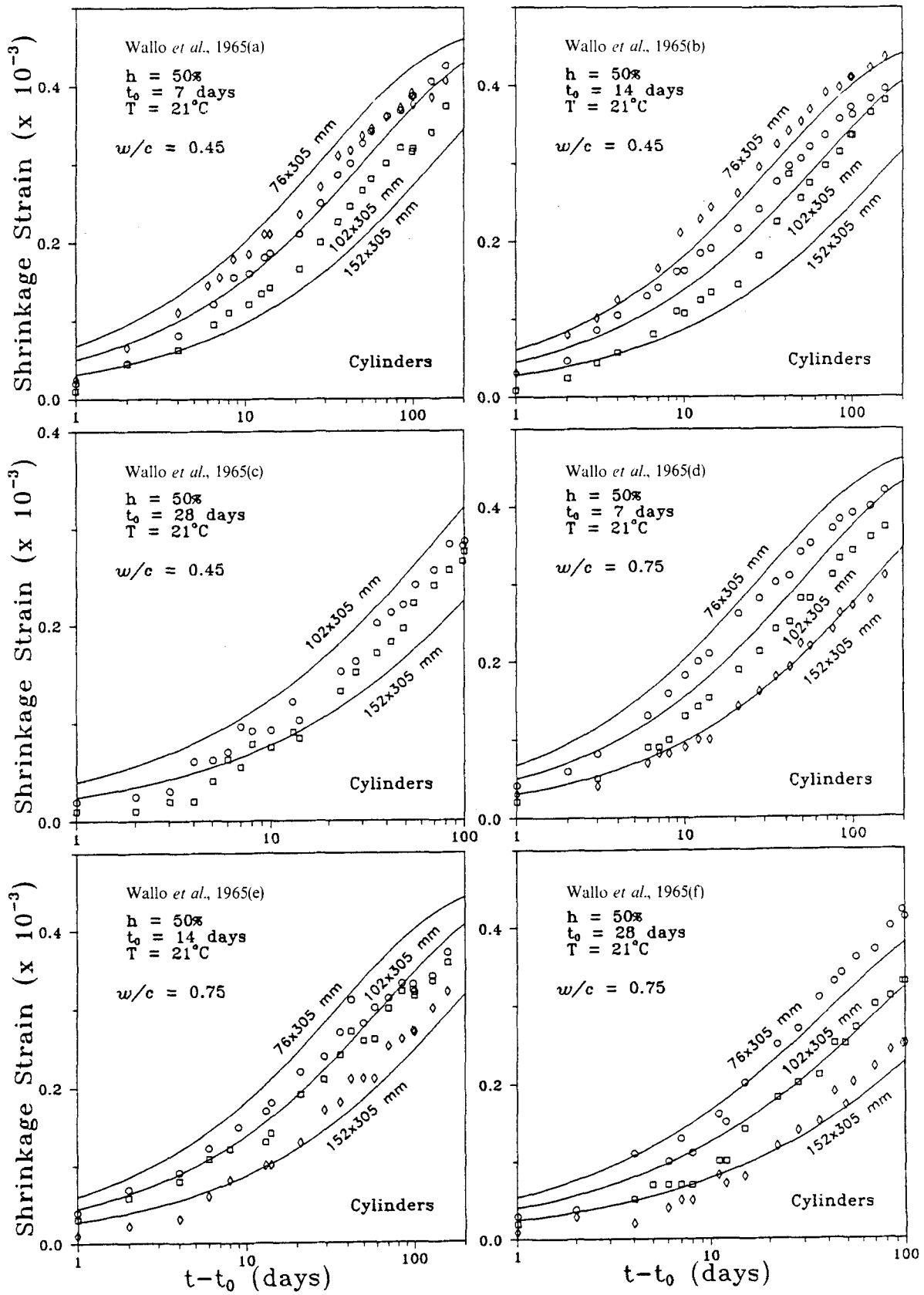Fig. 5 Predictions of shrinkage and data by L'Hermite *et al.*, L'Hermite and Mamillan and Rüsch *et al.*

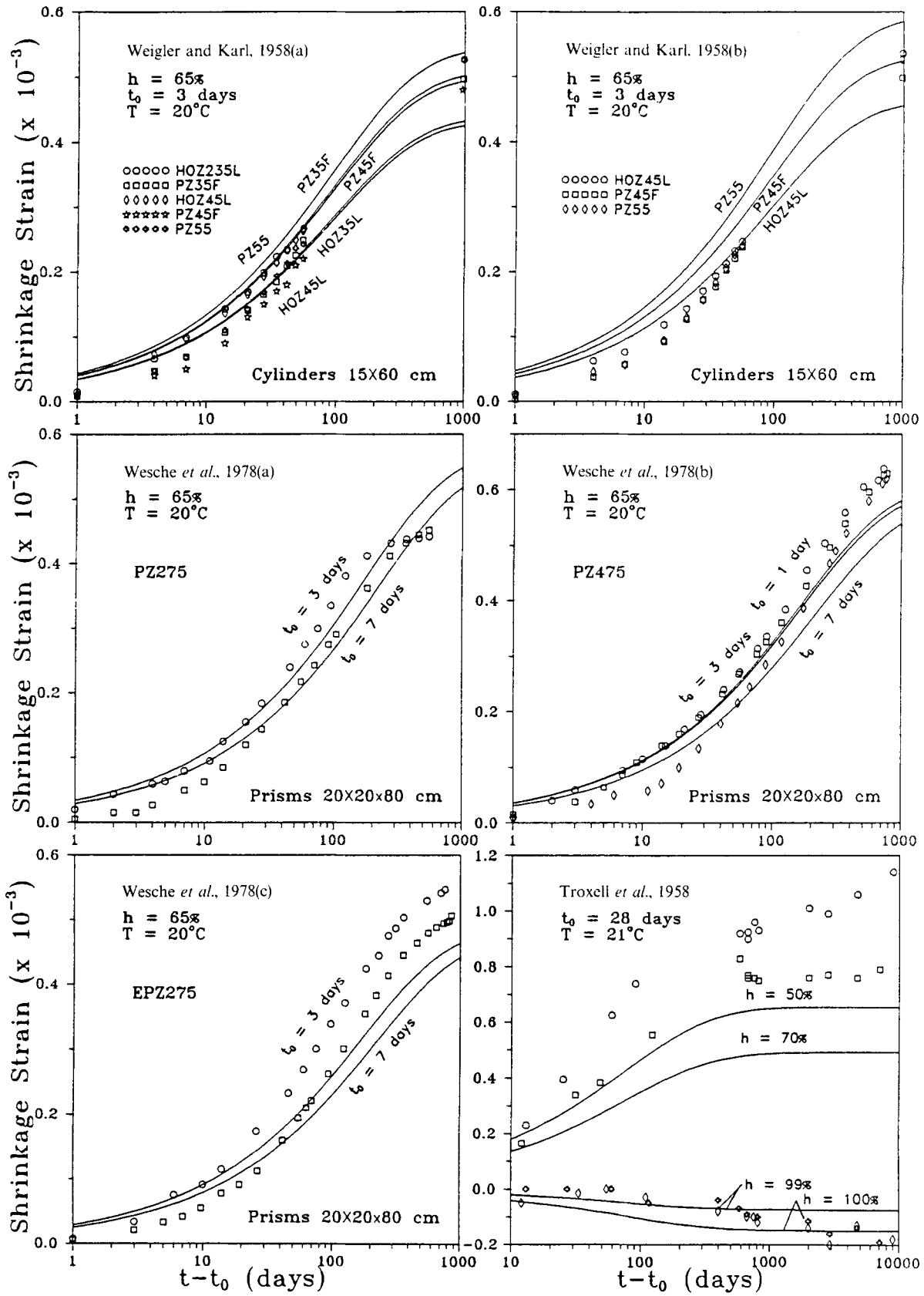Fig. 6 Predictions of shrinkage and data by Wallo *et al.*

Fig. 7 Predictions of shrinkage and data by Weigler and Karl, Wesche *et al.* and Troxell *et al.*
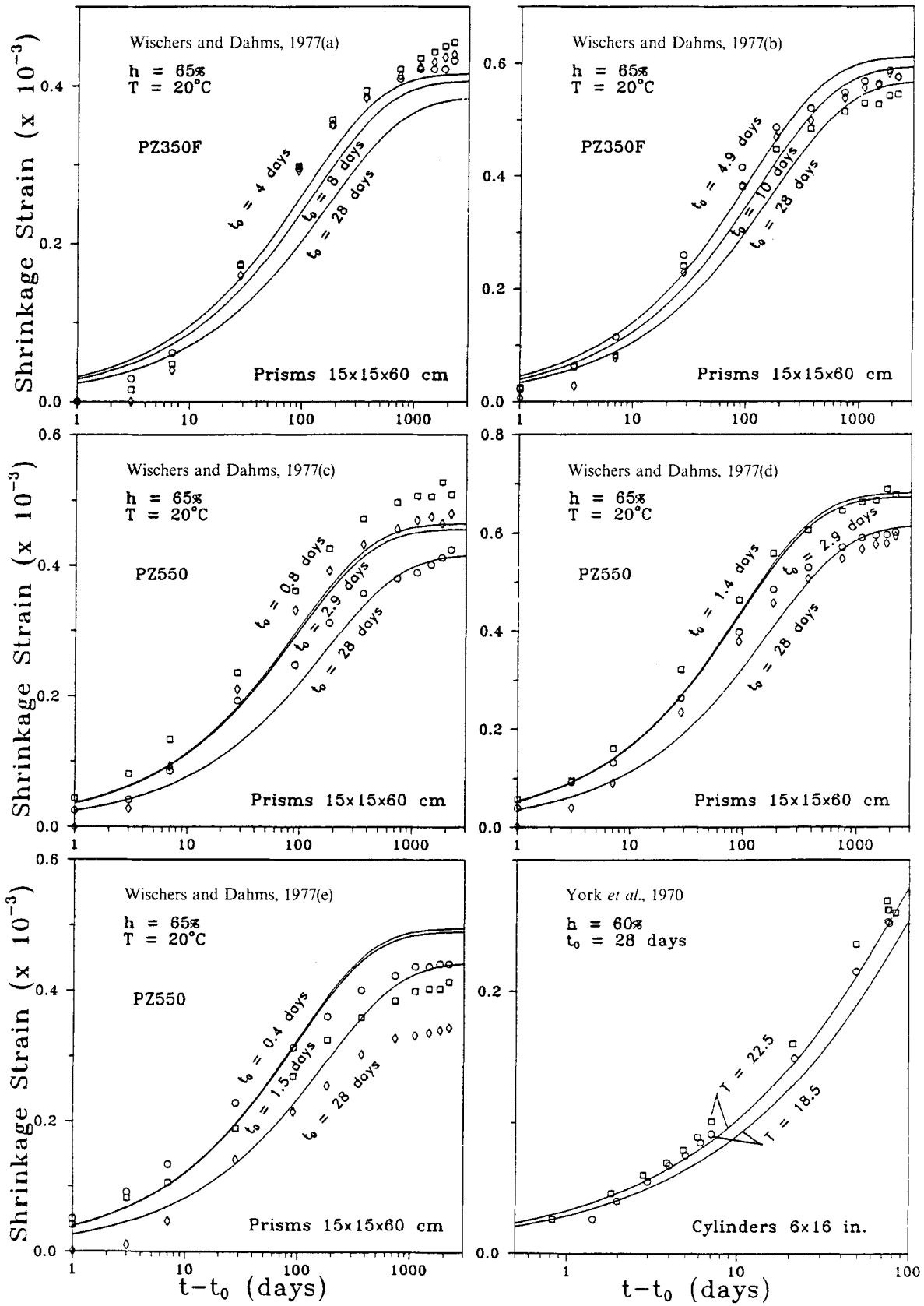
Fig. 8 Predictions of shrinkage and data by Wischers and Dahms and York *et al.*

Table 1 Coefficients of variation for deviations of formulae from hand-smoothed data for shrinkage $(\bar{\omega}_{all} = (\sum \bar{\omega}^2/N)^{1/2}$, where N = number of data-sets) as plotted in Figs 1–8

Individual data-sets				Data from each report or paper combined	
Test data	$\bar{\omega}$	Test data	$\bar{\omega}$	Test data	$\bar{\omega}$
Aschl and Stöckl	60.5	Troxell et al.	38.4	Aschl and Stöckl	60.5
Dreux and Gorisse	54.8	Kesler et al. (a)	21.3	Dreux and Gorisse	54.8
Espion and Wastiels	17.0	Kesler et al. (b)	21.4	Espion and Wastiels	17.0
Hansen and Mattock (a)	17.9	Kesler et al. (c)	24.7	Hansen and Mattock	17.3
Hansen and Mattock (b)	16.0	Kesler et al. (d)	26.5	Hilsdorf	10.9
Hilsdorf	10.9	Kesler et al. (e)	22.9	Hummel et al.	14.0
Hummel et al.	14.0	Wallo et al. (a)	17.4	Keeton	15.0
Keeton (a)	16.7	Wallo et al. (b)	21.6	Lambotte and Mommens	27.3
Keeton (b)	18.4	Wallo et al. (c)	24.4	L'Hermite et al.	54.8
Keeton (c)	18.1	Wallo et al. (d)	14.6	L'Hermite and Mamillan	53.6
Keeton (d)	12.3	Wallo et al. (e)	16.1	McDonald	33.1
Keeton (e)	8.4	Wallo et al. (f)	14.3	Ngab et al.	27.2
Keeton (f)	13.0	Weigler and Karl (a)	16.6	Rüsch et al. (1)	15.8
Keeton (g)	13.4	Weigler and Karl (b)	22.8	Rüsch et al. (2)	13.0
Lambotte and Mommens	27.3	Wesche et al. (a)	13.1	Stöckl	32.2
L'Hermite et al.	54.8	Wesche et al. (b)	16.7	Troxell et al.	38.4
L'Hermite and Mamillan (a)	38.2	Wesche et al. (c)	24.7	Kesler et al.	23.4
L'Hermite and Mamillan (b)	75.0	Wittmann, Bazant et al.	11.8	Wallo et al.	17.4
L'Hermite and Mamillan (c)	39.1	Wischers and Dahms (a)	19.1	Weigler and Karl	19.2
McDonald	33.1	Wischers and Dahms (b)	12.6	Wesche et al.	18.3
Ngab et al.	27.2	Wischers and Dahms (c)	21.8	Wittmann et al.	11.8
Rüsch et al. (1)	15.8	Wischers and Dahms (d)	11.8	Wischers and Dahms	18.2
Rüsch et al. (2)	13.0	Wischers and Dahms (e)	22.8	York et al.	12.3
Stöckl	32.2	York et al.	12.3		
	$\bar{\omega}_{all} = 27.0$			$\bar{\omega}_{all} = 30.5$	

predicted values from the hand-smoothed measured curves (see Table 1). The method of statistical analysis of the test data was described in detail on pp. 117–181 of Part VI of Bažant and Panula [1], and need not be described here again.

It must be admitted that much of the error of shrinkage seen in the figures may be systematic rather than random, and could probably be eliminated by a better theory, especially for the effect of composition and strength. But, lacking a better theory, we have no way to judge this question. Therefore one has to treat the entire error as statistical in nature, treating the deviation of our formulae from the data as a random variable. To avoid any possible subjective bias, each curve in each data-set is assigned the same weight.

9. PHYSICAL MECHANISMS INVOLVED AND UNDERLYING CONCEPTS

To the maximum extent possible, Equations 1–10 have been based on the latest physical concepts of shrinkage mechanism. These are as follows:

1. *Size effect.* According to the diffusion theory for drying [24] (not only linear diffusion theory but also non-

linear diffusion theory), τ_{sh} should be proportional to D^2 and inversely proportional to the diffusivity of concrete (Equation 4). There are, of course, several phenomena which to some extent spoil the diffusion-type size effect. These are the ageing of concrete, the change of creep due to a drop in moisture content, and the microcracking caused by drying. Analysis of test data, however, does not reveal any sufficiently systematic deviations from the present formulae based on diffusion theory. Anyhow, if these phenomena should be taken into account, it would not require abandoning diffusion theory but enhancing it with additional corrections.

2. *Initial asymptotic curve.* It further follows from the diffusion theory that the initial shape of the shrinkage curve ought to be proportional to $t^{1/2}$. This is again true for both linear and non-linear diffusion theories [24], and is not spoiled by ageing, cracking, creep or other phenomena, as has been shown. Careful measurements of the initial shrinkage [13] have verified this law with excellent accuracy.

3. *Final asymptotic curve.* It can further be deduced from diffusion theory, both linear and non-linear, that the final asymptotic value of the average shrinkage of the cross-section should be approached as a decaying exponential of a power function of time [24]. Although

this seems to agree reasonably well with the existing test data, experimental support of this aspect is weak, mainly because the measurements for very long durations are much more randomly scattered and also very scant.

4. *Effect of cross-section shape.* Due to the diffusive nature of drying, the rate of shrinkage, as indicated by the half-time of shrinkage, should depend approximately on the volume-to-surface ratio of the cross-section, with corrections [4] that can be established on the basis of the solutions of the diffusion equation, as indicated in Equation 5.

5. *Activation energy theory.* The basic physical processes in shrinkage are all thermally activated processes, obeying the rate process theory. This is true of the movement of water molecules through pores, which involves periodic breakages of adsorption bonds, as well as the effect of ageing of concrete, which is due to the chemical reaction of cement hydration. For this reason the rate coefficients involved in the shrinkage prediction formulae (Equation 1) should be proportional to an exponential of $-Q/RT$, where T = absolute temperature and Q = activation energy (see Equation 10).

6. *Effect of microcracking.* The non-uniformity of drying inevitably causes microcracking or macroscopic cracking. The consequence is that the observed mean shrinkage in a specimen is much less than the true free shrinkage of a small material element [25,26]. The effect of microcracking does not appear directly in the present equations, but it is contained empirically in the value of the coefficient $\varepsilon_{sh\infty}$. Without microcracking caused by non-uniform drying the value of $\varepsilon_{sh\infty}$ would be much larger, and much closer to the free shrinkage of a material element. In addition, and more importantly, the extent of microcracking is reflected in the difference between shrinkage and stress-induced shrinkage (also called drying creep), to be considered in Part III. The stress-induced shrinkage is largely (but not entirely) due to the reduction or complete suppression of microcracking caused by applied compressive stress.

10. ASYMPTOTIC FORMS OF PROPOSED TIME-CURVE

In the original BP model [1] the shrinkage time-curve was of the following type:

$$S(t) = \left[\frac{(t/\tau_{sh})^r}{1 + (t/\tau_{sh})^r}\right]^{1/2r} = \left[1 + \left(\frac{\tau_{sh}}{t}\right)^r\right]^{-1/2r} \quad (18)$$

in which the value $r = 1$ was used. For very short drying times t compared to τ_{sh} the denominator of the first expression in Equation 18 is approximately unity, and so

$$\text{for } t \ll \tau_{sh}: \quad S(t) \simeq \left(\frac{t}{\tau_{sh}}\right)^{1/2} \quad (\text{any } r) \quad (19)$$

which is what is required by diffusion theory [24]. Furthermore, noting that $(1 + \delta)^n = 1 + n\delta$ if δ is very small, one concludes from the second expression in

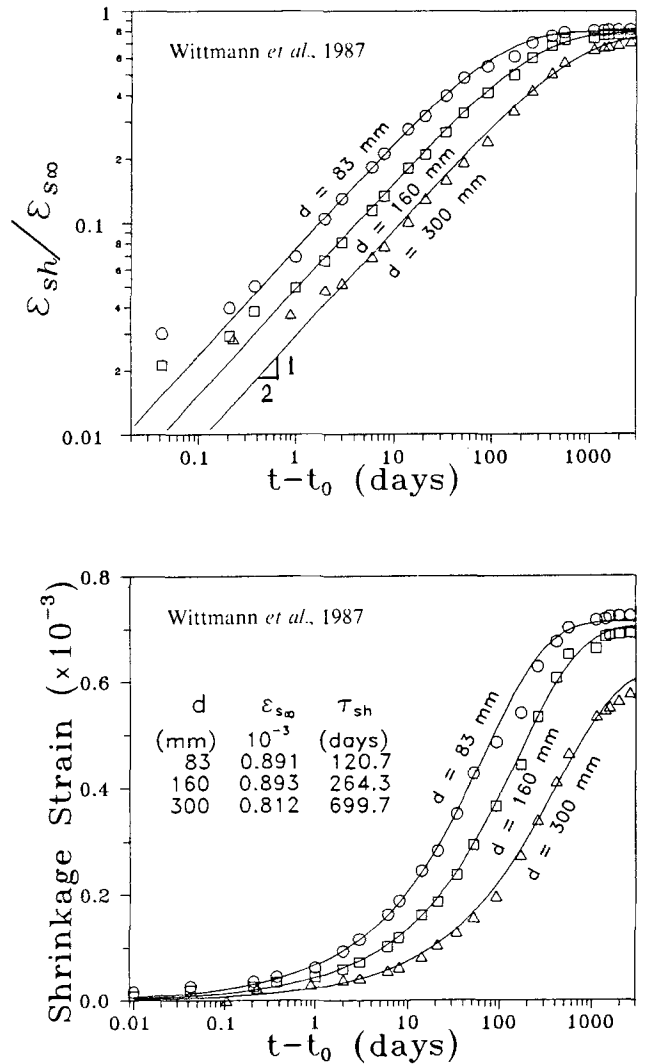Fig. 9 Individual optimum fits of tests by Wittmann *et al.*

Equation 18 that for very long drying times $S(t) \simeq [1 - (\tau_{sh}/t)^r/2r]$, that is

$$\text{for } t \gg \tau_{sh}: \quad 1 - S(t) \simeq \frac{1}{2}\frac{\tau_{sh}}{t} \quad (r = 1) \quad (20)$$

This asymptotic form, however, disagrees with the aforementioned consequence of diffusion theory. This is one reason why the function $S(t)$ used in the original BP model has been abandoned. As for experimental verification, there are not many data that would be sufficiently extensive for checking the final shape of shrinkage curves. The most extensive are those of Wittmann *et al.* [13], obtained as averages from 35 or 36 specimens. The optimum fit of these data, shown in Fig. 9, demonstrates that a very good fit is achieved. However, it must be admitted that the fit is only slightly better than that of Equation 18.

Now consider Equation 2, which reads $S(t) = \tanh x$ if one denotes $x = (t/\tau_{sh})^{1/2}$. For short drying times compared to τ_{sh}, i.e. $t \ll \tau_{sh}$, we have $\tanh x \simeq x$, which means that the initial asymptotic form in Equation 19, required by diffusion theory, is again verified by the present
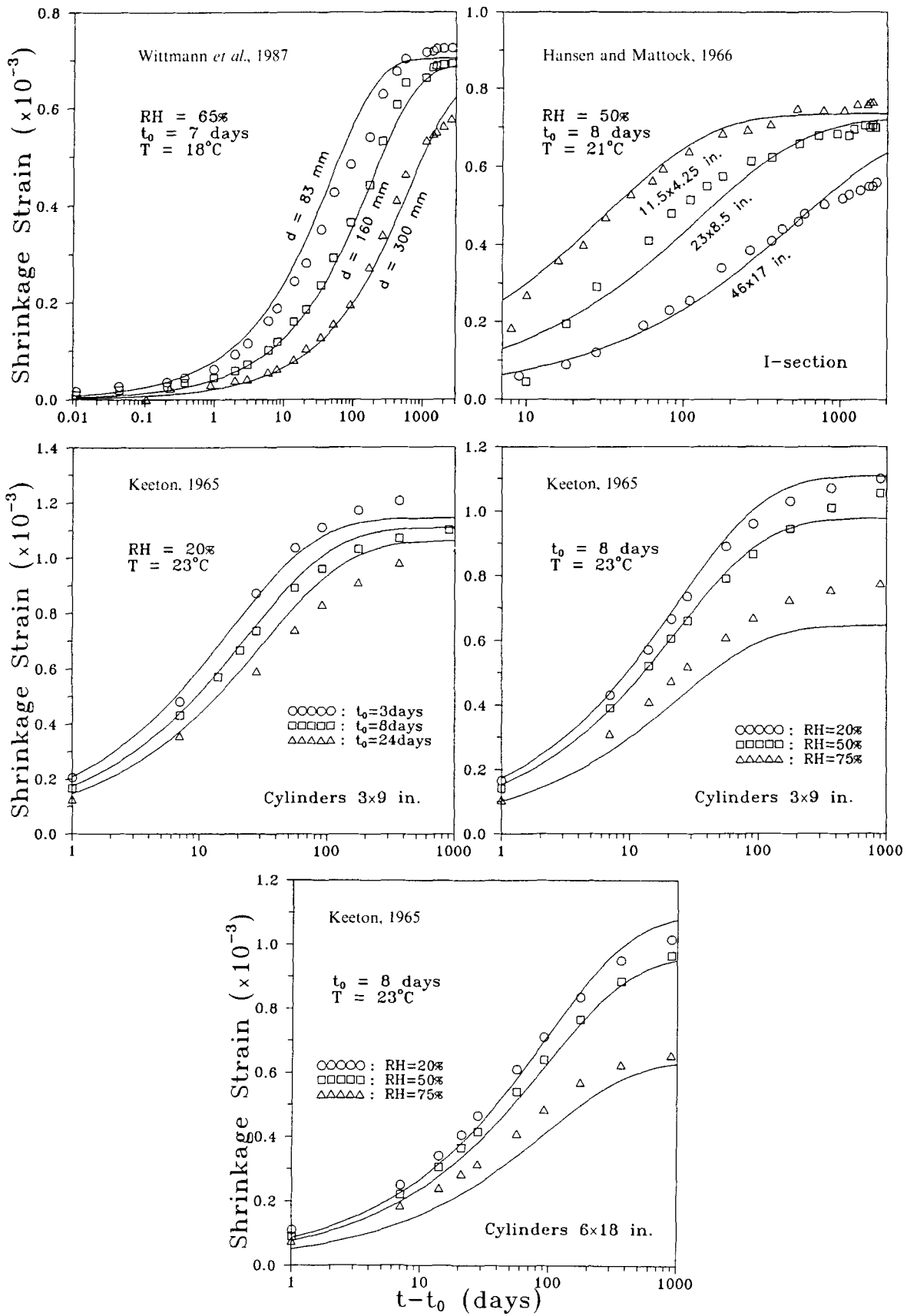
Fig. 10 Optimum fits of test data by Wittmann *et al.*, Hansen and Mattock and Keeton.

formula. Furthermore, for drying times very large compared to τ_{sh}, one has

for $\hat{t} \gg \tau_{sh}$: $\quad 1 - S(\hat{t}) = 1 - \tanh x = 1 - \dfrac{e^x - e^{-x}}{e^x + e^{-x}}$

$$= \frac{2e^{-2x}}{1 + e^{-2x}} \simeq 2e^{-2x}$$

$$= 2 \exp\left[-2\left(\frac{\hat{t}}{\tau_{sh}}\right)^{1/2}\right] \qquad (21)$$

This asymptotic form does agree with the aforementioned consequence of diffusion theory [24].

11. OPTIMUM FITS OF INDIVIDUAL DATA-SETS

The main error of the present model (Equations 1–15) stems from the errors in prediction of the material parameter values (Equations 11–15). If the material parameters are estimated separately for each data-set for one and the same concrete, much closer fits can be obtained. Such fits verify that the form of the present equations is correct. For example, if $\varepsilon_{s\infty}$ and τ_{sh} or $C_1(t_0)$ are optimized individually for each curve, the fits are as close as shown in Fig. 9. The parameter values for the optimum fits are listed in the figure legends. The less comprehensive or more scattered data-sets are insufficient to check the form of the shrinkage (Equations 1–10). Fig. 10 shows for several data how close the fits are when $\varepsilon_{s\infty}$ and $C_1(t_0)$ are optimized.

12. CONCLUSIONS

Although the presently proposed prediction model is justified by physical concepts to a larger extent that other models, it is still approximate. Nevertheless, it is in better agreement with experimental evidence than other models, and probably further improvement could hardly be achieved without an increase in complexity. The large body of data assembled in this part is a valuable yardstick for shrinkage prediction models of all kinds and should be utilized in future studies to determine their error statistics, which have to be established for any model proposed for practical use, even the most simple one.

APPENDIX: Basic information on shrinkage data used

Aschl and Stöckl [27]. After 28 days, specimens 15 cm × 15 cm × 30 cm were exposed to relative humidity 65% and temperature 20°C. Water:cement:sand:coarse aggregate ratio = 0.52:1:2.58:2.49; 28-day cube strength = 60.6 N mm^{-2}; cement (HOZ 450L) content 351 kg m^{-3}.

Dreux and Gorisse [15]. After 66 h curing, specimens 15 cm × 40 cm × 50 cm were allowed to dry at 21°C and 51% relative humidity. Cement content 400 kg m^{-3}, water:cement:sand:coarse aggregate ratio = 0.50:1:1.58:

2.84; 28-day cylinder strength 39.1 N mm^{-2} (average value).

Espion and Wastiels [21]. Specimens 15 cm × 15 cm × 60 cm cured 1 day in mould, then exposed at 60% relative humidity and 20°C. Water:cement:sand:coarse aggregate ratio = 0.48:1:1.55:3.38; 28-day cylinder strength = 36.0, 33.3 and 37.2 N mm^{-2}; ordinary Portland cement (ASTM type I) content 375 kg m^{-3}.

Hansen and Mattock [9]. Specimens drying at 50% relative humidity; length of cylinders of 10 to 61 cm diameter are 457, 559, 660, 864, 1067, 1270 and 1473 mm. ASTM type III cement content 303 kg m^{-3}, cured 2 days in mould and 6 days in fog at 70°F (21°C). Specimens exposed to drying at 8 days of age. Water:cement:sand: coarse aggregate ratio = 0.71:1:3.3:2.7. Maximum size of aggregate = $\frac{3}{4}$ in. (19 mm); 28-day cylinder strength 6000 psi (41.4 N mm^{-2}).

Hilsdorf [18]. Cylinders 20 cm × 80 cm were transferred to an environment of relative humidity 55% and temperature 20°C. Water:cement:sand:coarse aggregate ratio = 0.55:1:2.79:2.61; 28-day cube strength = 47.5 N mm^{-2}; cement (PZ475) content 337 kg m^{-3}.

Hummel et al. [12]. Cured 1 day in mould, then until age of 7 days under wet rugs at 20°C. After 7 days, cylinders 20 cm × 80 cm were transferred to an environment of relative humidity 65% and temperature 20°C. Water: cement:sand:coarse aggregate ratios = 0.55:1:2.79:2.61, 0.38:1:2.79:2.68, 0.45:1:2.79:2.68 and 0.55:1:2.79:2.69; 28-day cube strength = 31.7, 50.9, 41.7 and 49.4 N mm^{-2}; cement (PZ225) content 334, 350 and 345 kg m^{-3}, and cement (PZ425) content 334 kg m^{-3}, respectively.

Keeton [6]. Portland cement of ASTM type III, content 452 kg m^{-3}. Water:cement:sand:coarse aggregate ratio = 0.46:1:1.66:2.07; maximum size of aggregate = $\frac{3}{4}$ in. (19 mm); 28-day cylinder strength 6550 psi (45.2 N mm^{-2}). Temperature 73°F (23°C).

Kesler et al. [7]. Specimens drying at 70°F (20°C) and 50% relative humidity; exposed after moist curing for 28 days to drying. Type I Portland cement contents 396, 218 and 396 kg m^{-3}. Water:cement:sand:coarse aggregate ratios = 0.5:1:2:2.4 and 0.8:1:3.8:5.2; 28-day cylinder strengths = 6708, 3339 and 7883 psi (46.25, 23.02 and 54.35 MPa), respectively.

Lambotte and Mommens [28]. Cured 24 h in moulds, then exposed to 60% relative humidity and 20°C. High-strength Portland cement contents 300 and 375 kg m^{-3}. Water:cement:sand:coarse aggregate ratios = 0.55:1: 3.23:3.28 and 0.47:1:2.6:2.63; 28-day cube strengths 36.1 and 46.0 N mm^{-2}, respectively.

L'Hermite et al. [11]. Specimens 7 cm × 7 cm × 28 cm drying at 20°C. French type 400/800 cement content 350 kg m^{-3}, cured in water and exposed to drying at the age of 2 days. Water:cement:sand:coarse aggregate ratio = 0.49:1:1.75:3.07; 28-day cylinder strength 5365 psi (34.8 N mm^{-2}).

L'Hermite and Mamillan [10]. Specimens drying at 55% relative humidity and 20°C temperature. French (type I) cement content 350 kg m^{-3}, cured in water and exposed to drying at the age of 2 days. Water:cement:

sand:coarse aggregate ratio = 0.51:1:1.69:3.37. Seine gravel (siliceous calcite), maximum size of aggregate 20 mm. 28-day cylinder strength 5365 psi (34.8 N mm^{-2}).

McDonald [29]. After 78 days of wet curing, cylinders 6 in. × 16 in. (152 mm × 406 mm) were allowed to dry at 73°F (23°C) and 50% relative humidity. Portland cement type II, content 404 kg m^{-3}; limestone aggregate, maximum size of aggregate $\frac{3}{4}$ in. (19 mm). Water:cement:sand:coarse aggregate ratio = 0.425:1:2.03:2.62; average cylinder strength 7320 psi (50.5 N mm^{-2}).

Ngab et al. [19,20]. After 28 days of moist-room curing, specimens 3.5 in. × 3.5 in. × 10.5 in. (89 mm × 89 mm × 267 mm) were allowed to dry at 21°C and 60% relative humidity. Portland cement type I, content 290 and 581 kg m^{-3}; water:cement:sand:coarse aggregate ratios = 0.64:1:2.79:3.82 and 0.32:1:1.23:1.58; cylinder strength 4720 and 9520 psi (32.5 and 65.6 MPa), respectively.

Rüsch et al. [14]. Cylinders 20 cm × 80 cm, cured in humidity room at 99% relative humidity until age of 7 days, then exposed to 65% relative humidity and 20°C. Cement (PZ225) content 337 kg m^{-3}; water:cement:sand:coarse aggregate ratios = 0.55:1:2.82:2.65 and 0.55:1:3.22:3.04; 28-day cube strength 30.1 and 33.5 N mm^{-2}, respectively. Here $s/c = 2.82$, $g/c = 2.65$ and $f'_c = 30.1$ N mm^{-2} are the averages of $s/c = 2.79$, 2.81, 2.79, 2.87, 2.83, $g/c = 2.6$, 2.66, 2.61, 2.72, 2.67 and $f'_c = 28.8$, 30.1, 31.1, 27.6, 33.5 N mm^{-2}, respectively.

Rüsch et al. [30]. Cured 24 h in moulds, then at 100% relative humidity until age of 7 days, then exposed to 65% relative humidity and 20°C. Cement (PZ375) content 344 kg m^{-3}, cement (PZ475) content 401 kg m^{-3}; water:cement:sand:coarse aggregate ratios = 0.49:1:2.79:2.55 and 0.49:1:2.4:1.99; 28-day cube strength 56.4 and 51.7 N mm^{-2}, respectively.

Stöckl [31]. Cylinders 15 cm × 30 cm cured 24 h in moulds, then stored in moisture room until age of 7 days, then exposed to 65% relative humidity and 20°C. Cement (PZ275) content 360, 250, 360 and 250 kg m^{-3}; water:cement:sand:coarse aggregate ratios = 0.6:1:2.6:2.4, 0.6:1:4.27:3.95, 0.45:1:2.76:2.54 and 0.8:1:4.04:3.72; 28-day cube strength 21.4, 22.7, 28.2 and 13.6 N mm^{-2}, respectively.

Troxell et al. [22]. After 28 days curing, cylinders 4 in. × 14 in. (102 mm × 356 mm) were allowed to dry at temperature 70°F (21°C). Water:cement:sand:coarse aggregate ratio = 0.59:1:2:3.69; 28-day cube strength 2500 psi (17.2 N mm^{-2}); cement type I, content 320 kg m^{-3}; granite aggregate, maximum size of aggregate 1.5 in. (38 mm).

Wallo et al. [8]. Specimens exposed at 70°F (21°C) and 50% relative humidity. Cement type I, content 323 and 195 kg m^{-3}; water:cement:sand:coarse aggregate ratios = 0.45:1:3:3 and 0.75:1:4.8:5.9; cylinder strengths 5500 and 3000 psi (38 and 21 MPa), respectively.

Weigler and Karl [32]. Cylinders 15 cm × 60 cm at 65% relative humidity and 20°C. Cement content 350, 292 and 269 kg m^{-3} with different cement types; water:cement:sand:coarse aggregate ratios = 0.5:1:2.73:2.72, 0.6:1:3:3 and 0.65:1:3.3:2.9; 28-day cube strength [48.7, 48.0, 44.2,

52.8, 56.3], [40.3, 45.3] and 47.5 N mm^{-2}; cement type [HOZ35L, PZ35F, HOZ45L, PZ45F, PZ55], [HOZ45L, PZ45F] and PZ55, respectively.

Wesche et al. [23]. Specimens 20 cm × 20 cm × 80 cm cured 24 h in moulds, then in humidity room at 100% relative humidity under wet towels, then exposed to 65% relative humidity and 20°C. Cement (PZ275) content 336 kg m^{-3}, cement (PZ475) content 337 kg m^{-3}, cement (PZ275 plus 25% HUS) content 336 kg m^{-3}; water:cement:sand:coarse aggregate ratio = 0.55:1:2.79:2.6; 28-day cube strength 39.2, 54.9 and 38.3 N mm^{-2}, respectively.

Wischers and Dahms [33]. Specimens 15 cm × 15 cm × 60 cm cured in water until 2 h before the start of drying test, then exposed to 65% relative humidity and 20°C. Cement (PZ350F) content 325 kg m^{-3}, cement (PZ350F) content 410 kg m^{-3}, cement (PZ550) content 325 kg m^{-3}, cement (PZ550) content 410 kg m^{-3}, cement (PZ550) content 400 kg m^{-3}; water:cement:sand:coarse aggregate ratios = 0.48:1:2.93:2.93, 0.48:1:2.12:2.12, 0.48:1:2.93:2.93, 0.48:1:2.12:2.12 and 0.48:1:2.29:2.29; 28-day cube strengths 59.4, 54.7, 66.4, 59.9 and 71.1 N mm^{-2}, respectively.

Wittmann et al. [13]. Cured in moulds until the start of test at 18 ± 1°C. After 7 days, specimens were transferred to an environment of relative humidity 65 ± 5% and temperature 18 ± 1°C. Water:cement:sand:coarse aggregate ratio = 0.48:1:2.09:3.32; 28-day cylinder strength 4814 psi (33.2 N mm^{-2}); cement (CPN, which is approximately ASTM type I) content 350 kg m^{-3}. The numerical values of the readings were given [13], except for the recently measured readings at 2610 days of drying, at which the values of the measured strains for 160 mm diameter specimens were: 697, 635, 679, 598, 712, 752, 675, 657, 732, 754, 640, 728, 728, 674, 712, 665, 653, 744, 631, 680, 711, 744, 705, 696, 729, 719, 658, 684, 762, 678, 680, 684, 678, 692, 656 × 10^{-6} (mean = 0.000692); for the 83 mm specimens: 749, 640, 676, 715, 697, 777, 825, 829, 787, 664, 669, 701, 742, 627, 802, 657, 719, 795, 628, 761, 789, 613, 755, 686, 810, 764, 698, 641, 714, 752, 749, 794, 734, 736, 704, 664 × 10^{-6} (mean = 0.000725); for the 300 mm specimens: 596, 576, 562 × 10^{-6} (mean = 0.000578).

York et al. [34]. After 7 days of curing, cylinders 6 in. × 16 in. (152 mm × 406 mm) were allowed to dry at 21°C and 60% relative humidity. Portland cement type II, content 404 kg m^{-3}; limestone, maximum size of aggregate 0.5 in. (13 mm). Water:cement:sand:coarse aggregate ratio = 0.425:1:2.03:2.62; cylinder strength 6200 psi (42.8 N mm^{-2}).

ACKNOWLEDGEMENTS

REFERENCES

1. Bažant, Z. P. and Panula, L., 'Practical prediction of time-dependent deformations of concrete', Parts I and II: *Mater. Struct.* **11**(65) (1978) 307–328, Parts III and IV: *ibid.* **11**(66) (1978) 415–434, Parts V and VI: *ibid.* **12**(69) (1979) 169–183.

2. Tsubaki, T. *et al.*, 'Probabilistic models', in 'Mathematical Modeling of Creep and Shrinkage of Concrete', edited by Z. P. Bažant (Wiley, London, 1988) pp. 311–384.

3. Bažant, Z. P. and Raftshol, W. J., 'Effect of cracking in drying and shrinkage specimens', *Cement Concr. Res.* **12**(2) (1982) 209–226.

4. Bažant, Z. P. and Najjar, J., 'Non-linear water diffusion in non-saturated concrete', *Mater. Struct.* **5** (1972) 3–20.

5. Bažant, Z. P., Osman, E. and Thonguthai, W., 'Practical formulation of shrinkage and creep of concrete', *ibid.* **9**(54) (1976) 395–406.

6. Keeton, J. R., 'Study of creep in concrete', Technical Reports R333-I, R333-II, R333-III (US Naval Civil Engineering Laboratory, Port Hueneme, California, 1965).

7. Kesler, C. E., Wallo, E. M. and Yuan, R. L., 'Free shrinkage of concrete and mortar', T&AM Report No. 664 (Department of Theoretical and Applied Mechanics, University of Illinois, Urbana, 1966).

8. Wallo, E. M., Yuan, R. L., Lott, J. L. and Kesler, C. E., 'Sixth progress report on prediction of creep in structural concrete from short time tests', T&AM Report No. 658, Department of Theoretical and Applied Mechanics, University of Illinois, Urbana, 1965).

9. Hansen, T. C. and Mattock, A. H., 'Influence of size and shape of member on the shrinkage and creep of concrete', *ACI J.* **63** (1966) 267–290.

10. L'Hermite, R. G. and Mamillan, M., 'Influence de la dimension des éprouvettes sur le retrait', *Ann. Inst. Techn. Bâtiment Trav. Publics* **23**(270) (1970) 5–6.

11. L'Hermite, R. G., Mamillan, M. and Lefèvre, C., 'Nouveaux résultats de recherches sur la déformation et la rupture du béton', *ibid.* **18**(207–208) (1965) 323–360; see also International Conference on the Structure of Concrete (Cement and Concrete Association, London, England, 1968) pp. 423–433.

12. Hummel, A., Wesche, K. H. and Brand, W., 'Der Einfluss der Zementart, des Wasser-Zement-Verhältnisses und des Belastungsalters auf das Kriechen von Beton', Deutscher Ausschuss für Stahlbeton, Heft 146 (Ernst, Berlin, 1962) pp. 1–58.

13. Wittmann, F. H., Bažant, Z. P., Alou, F. and Kim, J. K., 'Statistics of shrinkage test data', *Cement Concr. Aggreg.* **9**(2) (1987) 129–153 and privately communicated latest unpublished measurements (1991).

14. Rüsch, H., Kordina, K. and Hilsdorf, H. K., 'Versuche über das Kriechen des Betons', Deutscher Ausschuss für Stahlbeton, Heft 146 (1962).

15. Dreux, G. and Gorisse, F., 'Fluage des bétons soumis jeunes à un gradient de contrainte', *Ann. Inst. Techn. Bâtiment Trav. Publics* (326), série béton No. 144 (March 1975).

16. Bažant, Z. P., 'Prediction of concrete creep effects using age-adjusted effective modulus method', *ACI J.* **69** (April 1972) 212–217.

17. Bažant, Z. P. and Najjar, L. J., 'Comparison of approximate linear methods for concrete creep', *J. Struct. Division ASCE* **99** (ST9) (September 1973) 1851–1874.

18. Hilsdorf, H. K., 'Unveröffentlichte Versuche an der MPA München', private communication (1980).

19. Ngab, A. S., Nilson, A. H. and Slate, F. O., 'Behavior of high strength concrete under sustained compressive stress', Report No. 80-2, Department of Structural Engineering (Cornell University, Ithaca, New York, 1980).

20. *Idem*, 'Shrinkage and creep of high strength concrete', *ACI J.* **78**(4) (1981) 255–261.

21. Espion, B. and Wastiels, J., 'Creep and shrinkage tests carried out within the research program FRFC–FKFO 2.90001.80 on the behavior of partially prestressed concrete beams under long term sustained loading', Research Report (Brussels Free University, Brussels, Belgium, 1989).

22. Troxell, G. E., Raphael, J. E. and Davis, R. W., 'Long-time creep and shrinkage tests of plain and reinforced concrete', *Proc. ASTM* **58** (1958) 1101–1120.

23. Wesche, K. H., Schrage, I. and von Berg, W., 'Versuche zum Einfluss des Belastungsalters auf das Kriechen von Beton', Deutscher Ausschuss für Stahlbeton, Heft 295 (1978).

24. Bažant, Z. P. and Kim, J.-K., 'Consequences of diffusion theory for shrinkage of concrete', *Mater. Struct.* **24** (1991) 323–326.

25. Bažant, Z. P. and Chern, J. C., 'Strain-softening with creep and exponential algorithm', *J. Engng Mech. ASCE* **111**(EM5) (1985) 391–451.

26. *Idem*, 'Stress-induced thermal and shrinkage strains in concrete', *ibid.* **113**(10) (1987) 1493–1511.

27. Aschl, H. and Stöckl, S., 'Wärmedehnung, E-Modul, Schwinden, Kriechen und Restfestigkeit von Reaktorbeton unter einachsiger Belastung und erhöhten Temperaturen', Deutscher Ausschuss für Stahlbeton, Heft 324 (1981).

28. Lambotte, H. and Mommens, A. L., 'L'évolution du retrait du béton en fonction de sa composition et de l'âge', Technical Report, groupe de travail GT 22 (Centre national de recherches scientifiques et techniques et pour l'industrie cimentière, Bruxelles, 1976), and privately communicated unpublished data (1978).

29. McDonald, J. E., 'Time-dependent deformation of concrete under multiaxial stress conditions', Technical Report C-75-4 (Concrete Laboratory, US Army Engineering Waterways Experiment Station, Vicksburg, Miss., 1975).

30. Rüsch, H., Sell, R., Rasch, Ch., Grasser, E., Hummel, A., Wesche, K. and Flatten, H., 'Festigkeit und Verformung unbewehrten Betons unter Dauerlast', Deutscher Ausschuss für Stahlbeton, Heft 198 (1968).

31. Stöckl, S., 'Versuche zum Einfluss der Belastungshöhe auf das Kriechen von Beton', *ibid.* Heft 324 (1981).

32. Weigler, H. and Karl, S., 'Kriechen des Betons bei frühzeitiger Belastung', *Betonwerk und Fertigteiltechnik* H9/81 (1981) and privately communicated unpublished data.

33. Wischers, G. and Dahms, J., 'Kriechen von frühbelastetem Beton mit höher Anfangsfestigkeit', *Beton 27*, Heft 2 und 3 (1977).

34. York, G. P., Kennedy, T. W. and Perry, E. S., 'Experimental investigation of creep in concrete subjected to multiaxial compressive stresses and elevated temperatures', Research Report 2864-2 to Oak Ridge National Laboratory (Department of Civil Engineering, University of Texas, Austin, June 1970); see also 'Concrete for Nuclear Reactors', American Concrete Institute Special Publication No. 34 (1972) pp. 647–700.

RESUME

Modèle amélioré de prédiction des déformations du béton en fonction du temps: 1ère partie – Retrait

Ce rapport est le premier d'une série présentant un nouveau modèle de prédiction du fluage et du retrait du béton dénommé, pour abréger, modèle BKP. Ce modèle représente une mise à jour et une amélioration du modèle BP décrit dans ce journal en 1978/79. Des données expérimentales ultérieures disponibles dans la littérature, en même temps qu'une meilleure connaissance des concepts et mécanismes physiques, ont permis ce progrès. Ce premier rapport présente un modèle de prédiction pour une contrainte de retrait moyenne dans les sections transversales de longs éléments, qui prend en compte l'influence de l'humidité ambiante, l'épaisseur effective de l'élément, l'influence de la forme de la section, de l'âge au début du séchage et de la température. On justifie l'expression de base des formules de retrait par la théorie de la diffusion non linéaire pour la circulation de l'humidité dans le béton. De vastes comparaisons avec d'importantes données d'essai prises dans la littérature – en tout 23 séries d'essai – ont montré que les prédictions étaient meilleures qu'avec les modèles précédents. On donne aussi des statistiques de prédiction. L'erreur de prédiction principale provient de l'évaluation des paramètres de retrait à partir de la composition et de la résistance du béton. Si l'on dispose de données de retrait limité, les prédictions peuvent être considérablement améliorées.